



Steering Graphene Quantum Dots in Living Cells: Light up the Nucleolus

Journal:	<i>Journal of Materials Chemistry B</i>
Manuscript ID	TB-ART-11-2015-002474.R1
Article Type:	Paper
Date Submitted by the Author:	14-Dec-2015
Complete List of Authors:	<p>Wang, Xiaojuan; China University of Petroleum (East China), Wang, Yanan; China University of Petroleum (East China) He, Hua; university of petroleum, Centre of Bioengineering and Biotechnology Chen, Xin; China University of Petroleum (East China) Sun, Xing; China University of Petroleum, Centre for Bioengineering and Biotechnology Sun, Yawei; university of petroleum, Centre of Bioengineering and Biotechnology Zhou, Guangjun; Shandong University, State Key Laboratory of Crystal Materials Xu, Hai; university of petroleum, Centre of Bioengineering and Biotechnology Huang, Fang; China University of Petroleum, Center for Bioengineering and Biotechnology</p>



Journal Name

ARTICLE

Steering Graphene Quantum Dots in Living Cells: Light up the Nucleolus

Received 00th January 20xx,
Accepted 00th January 20xx

Xiaojuan Wang,^{*ab} Yanan Wang,^b Hua He,^{ab} Xin Chen,^b Xing Sun,^b Yawei Sun,^{ab} Guangjun Zhou,^c Hai Xu^{ab} and Fang Huang^{*ab}

DOI: 10.1039/x0xx00000x

www.rsc.org/

Although nucleolus is an important subnuclear structure, there are very rare dyes available on the market for nucleolar imaging. On the other side, subcellular organelles delivery presents a common stumbling block for many nanomaterial-based applications, including intracellular structure fluorescence staining. We now introduce a novel luminescent graphene quantum dot (nGQD), which is able to selectively light up the nucleoli of living cells, to address these challenges. Investigations on subcellular localization of different GQDs have demonstrated that the positively charged surface and the ultra-small size are the key parameters for nucleoli-rich distribution of nanomaterials, which is of importance for transferring this strategy to other nanoparticles. The novel nGQD has great potentials to be applied as a nucleolar stain or an efficient gene/drug carrier.

Introduction

Studies of biological processes often require the staining of cell organelles. In spite of various commercial subcellular targeting dyes, there are very rare stains for nucleolar imaging available on the market.¹ Nucleolus is an important subnuclear structure and its architecture changes dynamically along with the physiological and the pathological situation. Although the biological roles of nucleolus have yet to be fully explicated, it is widely accepted that nucleolus is the key site where ribosomal RNAs are synthesized and processed.²⁻⁴ The nucleolar dysmorphology has been taken as a diagnostic reference to detect malignant lesions.⁵

In order to achieve selective visualization of the nucleoli, specific staining methods have been explored. For example, the nucleolar organizer regions (NORs) have been highlighted by a silver method exploiting the argyrophilic nature of a group of certain nucleolar proteins, which allows the contrast staining of the nucleolus under light microscopy.⁶ Taking advantage of the high sensitivity of fluorescence microscopy, several groups of fluorophores for nucleolus staining have

been developed, including (a) metal coordination complexes containing iridium, europium, ruthenium, and lanthanide,^{1, 7-11} (b) low molecular weight organic probes,¹²⁻¹⁵ (c) intramolecularly linked metal complexes,^{16, 17} and (d) ligand modified quantum dots.¹⁸ However, the organic dyes often require multi-step synthesis and suffer from photobleaching, while the potential toxicity of heavy metal in quantum dots limits their living cells application. Furthermore, although the functional nanoparticles have been extensively studied, the subcellular organelles delivery still remain a challenge, which limits their biological applications. It is therefore desirable to explore novel fluorophores, especially fluorescent nanoparticles, for specific nucleoli staining.

Graphene quantum dot (GQD) is a relatively young member in the family of carbon-based nanomaterials. Relying on the small size (2-40nm), good water solubility, and low cytotoxicity, it has attracted intensive research interests.¹⁹⁻²¹ By varying the size of graphene, the bandgap of graphene can be tuned from zero to that of benzene to get many interesting phenomena. Small GQDs show different photo-luminescence depending on their sizes and the chemical groups at their edge, which arises from quantum confinement and edge effects.¹⁹⁻²¹ The tunable intrinsic fluorescence of GQDs have been used to label various types of cells, including normal mammalian cells, cancer cells, and stem cells.²²⁻²⁸ In most studies bare GQDs are found to localize only in the cytoplasm. Although the GQDs synthesized by Dong et al were reported to diffuse through the whole cells, there was no evidence showing the cell organelles targeting accumulation.²⁶ The capability of GQDs to label certain subcellular structures has yet to be explored. Here, we report a novel GQD for lighting up the nucleoli in living cells. It is shown that by modifying the carboxyl acid groups on the surfaces of ultra-small GQDs with diamine, we are able to

^a State Key Laboratory of Heavy Oil Processing, China University of Petroleum (East China), Qingdao 266580, China;
Email: fhuang@upc.edu.cn

^b Centre for Bioengineering and Biotechnology, China University of Petroleum (East China), Qingdao 266580, China;
Email: xwang@upc.edu.cn

^c State Key Laboratory of Crystal Materials, Shandong University, Jinan 250100, China

† Electronic Supplementary Information (ESI) available: XPS C1s analysis of nGQD and cGQD, FL emission spectra of nGQD and cGQD at various excitation wavelength, gel electrophoresis of nGQD and cGQD, confocal laser scanning microscopy images of MCF-7 and HeLa cells labelled with nGQD, the MTT cell viability of HepG2 cells treated with nGQD and cGQD, and nGQD-stained HepG2 cells showing different number of nucleoli. See DOI: 10.1039/x0xx00000x

modulate the intracellular localization of GQD from cytoplasm only to a nucleoli-rich distribution. The key parameters for the specific organelle targeting are also discussed. The novel GQD has great application potentials as a nucleolus stain or a fluorescent drug/gene carrier.

Materials and Methods

Chemicals and materials

Carbon black (Vulcan CX-72) was obtained from Carbot Co., China. SOCl_2 and 1,2-ethylenediamine were obtained from Alfa Aesar Chemical Co., China. High-glucose Dulbecco's modified Eagle's medium (DMEM) and fetal bovine serum (FBS) were purchased from Life Technologies. SYTO RNA-Select was purchased from Molecular Probes. 3-(4,5-Dimethylthiazol-2-yl)-2,5-diphenyltetrazolium bromide (MTT) assay kit was purchased from Shanghai Sangon Biotech Co. All chemicals were used as received without further purification. All solutions were prepared with ultra-pure water ($\geq 18.2 \text{ M}\Omega$, Millipore, USA) or 0.01 M phosphate buffer saline (PBS, pH 7.4) unless otherwise specified.

nGQD synthesis

cGQD was synthesized as previously described.^{29, 30} 0.2g of as-prepared cGQD was mixed with 10mL of SOCl_2 and reacted at 80°C for 10 h. The product was vacuum-distilled to remove excess SOCl_2 and then reacted with 10 mL of 1,2-ethylenediamine at 80°C for 10 h. The resulting mixture was subsequently vacuum-distilled to remove most of the excess 1,2-ethylenediamine and washed with ethanol. The obtained black powder was dissolved in ultra-pure water and the solution was repeatedly dialyzed against water in a dialysis bag (retaining molecular weight = 1000 Da) for 24 h to obtain a pure nGQD solution.

Characterization

X-ray Photoelectron Spectroscopy was investigated by using a ESCALAB 250 spectrometer. FTIR spectra were obtained using a Nicolet 6700 FTIR spectrometer. Ultraviolet–visible (UV-Vis) spectra were obtained using a Shimadzu UV-2450 spectrophotometer. Fluorescence spectra were collected using a Hitachi F-2500 fluorescence spectrophotometer. High-resolution transmission electron microscopic (HRTEM) images were recorded on a JEM-2100 electron microscope at 200 kV. Atomic force microscopic (AFM) images were obtained using a Nanoscope IV Multimode AFM (Digital Instruments, Santa Barbara).

Cell culture

Cells were cultured in a DMEM medium supplemented with 10% FBS in a humidified 5% CO_2 atmosphere inside an incubator at 37 °C. The cells were harvested from 90% confluent cell culture plates and were resuspended in fresh complete medium before plating.

Cell imaging

For living cell imaging, the cells (1×10^5) were seeded into a glass bottomed culture dish and precultured for 24 h. Then the culture medium was discarded. The cells were washed thrice with PBS, and incubated with GQDs (400 $\mu\text{g}/\text{mL}$) for 5 h. After washing thrice with PBS, the cells were directed scanned with confocal microscope (Nikon AI, Nikon, Japan).

For the colocalization experiment, the cells were first incubated with nGQD for 5 h, then 500nM of SYTO RNA-Select dye for 20min. After washing with PBS thrice, the cells were fixed for 20 min in 200 μL of 4% paraformaldehyde, washed with PBS, and then applied for confocal microscopy assay.

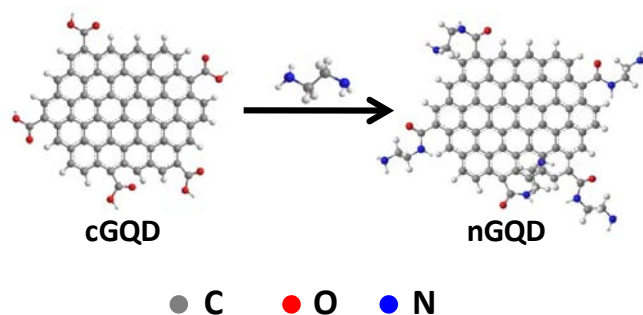
nGQD was excited with 405 nm laser and the fluorescence signal was collected between 425 ~ 475nm. cGQD and SYTO RNA-Select were excited with 488 nm laser and the fluorescence signal was collected between 500 ~ 530nm.

Cell viability assay

The in vitro cytotoxicity of nGQD in comparison with cGQD was evaluated by MTT cell viability assay. The cells were seeded on 96-well plates at 2×10^4 cells/well in 100 μL of medium containing 10% FBS. The plates were incubated for 24 h at 37 °C in a humidified 5% CO_2 atmosphere. On the day of experiments, the cells were washed with PBS buffer and incubated with fresh medium containing GQDs. The cells were then incubated with GQDs at 37 °C for 24 h. The wells containing cells without GQDs served as the control. Subsequently, 20 μL of MTT solution (5 mg/mL) was added to each well, and the plates were incubated at 37 °C for 4 h. The precipitated formazan was dissolved in 150 μL of dimethyl sulfoxide. The absorbance of each sample at 570 nm was measured using a microplateautoreader (Molecular Devices, M2e). The cell viability ratio was calculated using $A_{570} / A_{0, 570}$ (control).

Results and Discussion

Two groups of GQDs were investigated in this work. Firstly, GQDs containing carboxyl acid groups on the surfaces, named cGQD, were prepared as reported.^{29, 30} cGQD had been carefully characterized in our previous work as single-layered material with an average diameter of 2.3 nm. Secondly, cGQD was reacted with SOCl_2 followed by 1,2-ethylenediamine to produce the surface modified GQDs, named nGQD (Scheme 1).



Scheme 1 Schematic illustration of nGQD synthesis.

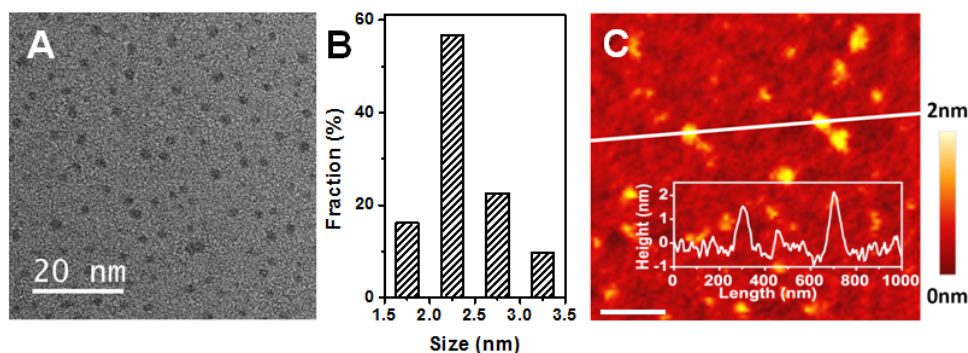


Fig. 1 HRTEM image (A), diameter distribution (B), AFM image and height profile (C, scale bar is 200 nm) of nGQD.

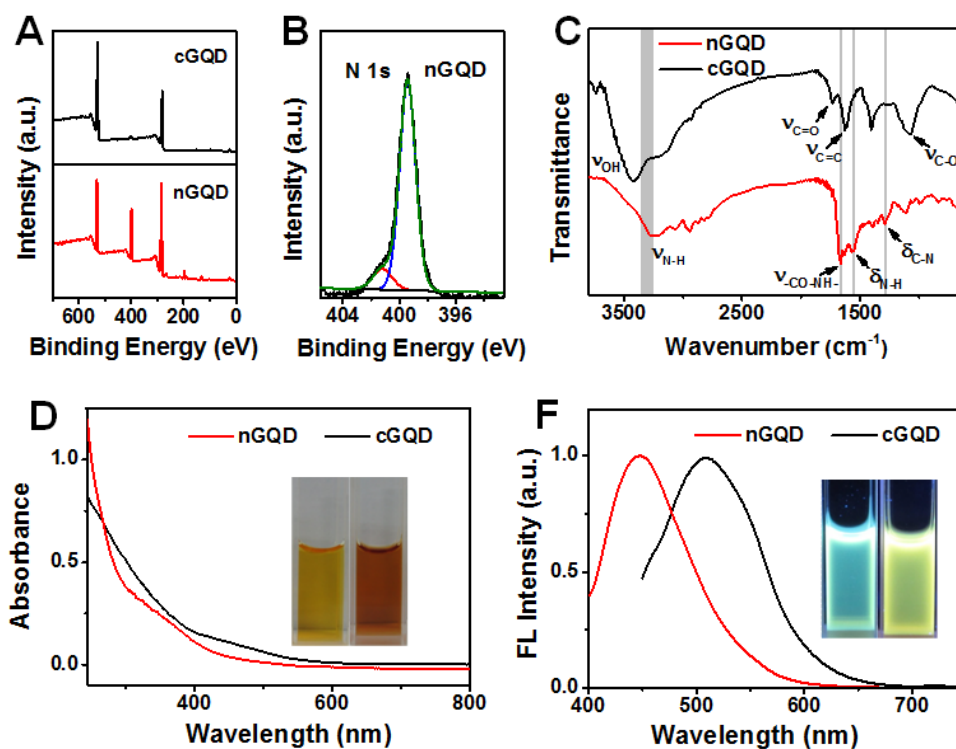


Fig. 2 Spectroscopic characterization of nGQD and cGQD. (A, B) X-ray photoelectron spectra analysis. (C) Fourier transform infrared spectroscopy. (D) UV-Vis absorption spectra. The inset is the photographs of nGQD (left) and cGQD (right) aqueous suspensions in day light. (E) Fluorescence emission spectra. The excitation wavelength is 380 nm. The inset shows the images of nGQD (left) and cGQD (right) aqueous suspensions under 365 nm UV light.

HRTEM images showed that the diameter of as-synthesized nGQD ranged between 1.5 to 3.5 nm with an average of 2.5 nm (Figs. 1A and B). As shown by atomic force microscopy (AFM, Fig. 1C), the topographic height of nGQD was around 1.7 nm. Although due to the connection of diamine slight increases in the morphology parameters were observed, the size of nGQD was kept at an ultra-small level, facilitating the cellular uptake and intracellular transport. The homogeneous

distribution of nGQD in both HRTEM and AFM images indicated that the surface modification procedure did not induce any aggregation, which is important for the subcellular targeting application.

X-ray photoelectron spectroscopy (XPS) and fourier transform infrared spectroscopy (FTIR) were carried out to check the composition of GQDs. Compared to the XPS survey spectrum of cGQD a distinct peak at 399.5 eV corresponding to

nitrogen was observed in the spectrum of nGQD, substantiating the successful diamine coupling (Fig. 2A). The prominent increase of oxygenated and nitrogenated carbon (286.3 to 286.7 eV) content in nGQD also verified the surface modification (Fig. S1). In addition, the high resolution N1s analysis revealed that both amide (399.4 eV) and protonated amine (401.2 eV) nitrogen were present in nGQD (Fig. 2B). In the FTIR spectra new peaks, assigned to the stretching vibration of N-H ($3300\text{--}3500\text{ cm}^{-1}$) and stretching of C-N (1280 cm^{-1}) and N-H (1560 cm^{-1}), appeared in nGQD due to the attached diamine. In addition, characteristic amide-carbonyl (NH-CO) stretching vibration was observed at 1660 cm^{-1} , implying the formation of amide groups in nGQD.

nGQD was further evaluated using various spectroscopic methodologies. UV-Vis scan results (Fig. 2D) showed that no obvious absorption peak can be observed in either cGQD or nGQD. The broad absorption band shifted from $\sim 320\text{ nm}$ in cGQD to $\sim 270\text{ nm}$ in nGQD due to the surface passivation of diamine.³¹ Both GQDs emitted visible fluorescence under the portable UV light and the colour of the photoluminescence was blue and green, respectively, for nGQD and cGQD. The fluorescence emission spectra indicated that both GQDs exhibited excitation-dependent photoluminescence behaviour (Fig. S2), which is common for the carbon nanomaterials.¹⁹⁻²¹ When excited at 380 nm , cGQD gave out an emission peak at 515 nm , which shifted to 447 nm in the spectrum of nGQD (Fig. 2F). Experimental assessment revealed that the quantum yield obtained a dramatic increase from 1.8% of cGQD to 13.1% of nGQD (using quinine sulphate as a reference). Similar hypsochromic shift of fluorescence emission as well as the quantum yield enhancement had been reported for the carbon dots modified with alkylamines, which was attributed to the combined effects of suppressed non-radiative process by passivating the initial carboxylic groups and the extension of the integrity of π conjugate through the cyclic structure formed by protonated amine group.^{31, 32} Gel electrophoresis (Fig. S3) demonstrated that cGQD migrated towards the anode while nGQD migrated towards the cathode under the same electric field after loaded in the middle line of the same gel, indicating the opposite electrical nature of these two kinds of GQDs.

In order to investigate the intracellular targeting specificity of nGQD and compare with cGQD, fluorescence imaging was conducted using 3 cell lines, human liver carcinoma cell line HepG-2, breast cancer cell line MCF-7, and human cervical cancer cell line HeLa. After incubation with nGQD or cGQD ($400\text{ }\mu\text{g/mL}$) for 5 h at 37°C , the GQD-stained cells were scanned with confocal microscopy. As shown in Fig. 3, in both cases the luminescence of GQDs were observed inside of the cells, indicating an efficient permeating ability of both nGQD and cGQD. However, the fluorescence of cGQD could only be detected in the cytoplasm, leaving a completely blank nucleus area in each cell. As a sharp contrast bright luminescent spots were evident within the nuclei region of the nGQD-loaded cells. Furthermore, the luminescence intensity of the glowing spots was about 1.8 times as high as that in the cytoplasm of the same cell, substantiating a more specific distribution of

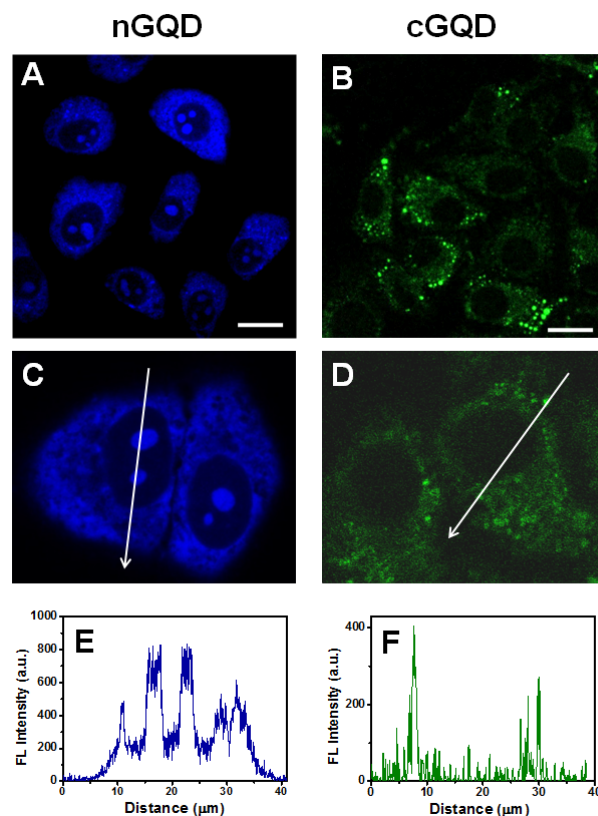


Fig. 3 Cellular uptake of (A) nGQD and (B) cGQD ($400\text{ }\mu\text{g/mL}$) by live HepG2 cells after incubation for 5 h at 37°C . Scale bar is $20\text{ }\mu\text{m}$. (C) and (D) are magnified view of nGQD- and cGQD-loaded cells, respectively; (E) and (F) are quantified fluorescence intensity profile along the lines shown in (C) and (D), respectively. For nGQD, $\lambda_{\text{ex}} = 405\text{ nm}$ and the fluorescence signal is collected between 425 nm and 475 nm . For cGQD, $\lambda_{\text{ex}} = 488\text{ nm}$ and the fluorescence signal is collected between 500 nm and 530 nm .

nGQD. Similar intracellular localization of nGQD was achieved in living MCF-7 and HeLa cells (Fig. S4), where the fluorescence of nGQD was found not only in the cytoplasm but also as bright spots inside of the nuclei region.

The nGQD-labelled cells were further loaded with commercial nucleolus stain SYTO RNA-Select and then imaged with confocal microscope. As shown in Fig. 4, the bright spots observed in the nGQD channel colocalized exactly with those obtained in the SYTO RNA-Select channel, which was further verified by the consistent quantified luminescence intensity profile along the white line in the merged image. This result strongly suggested that the luminescent spots observed inside of the nuclei region in the nGQD-loaded cells were related to the nGQD localized at the nucleoli.

It was known that the number and size of the nucleoli are varying between distinct cell lines and different mitotic stages. As was evident from the images (Fig. S4 and S6), the diversity of different cells lines and cells at various stages of nucleolar fusion could be easily differentiated after staining with nGQD, offering important information for biological analysis. It was therefore demonstrated that nGQD could be applied as a selective stain to light up the nucleoli in living cells.

The specific luminescence of nGQDs in the nucleoli may be caused by either the accumulation of nGQDs in the nucleolar

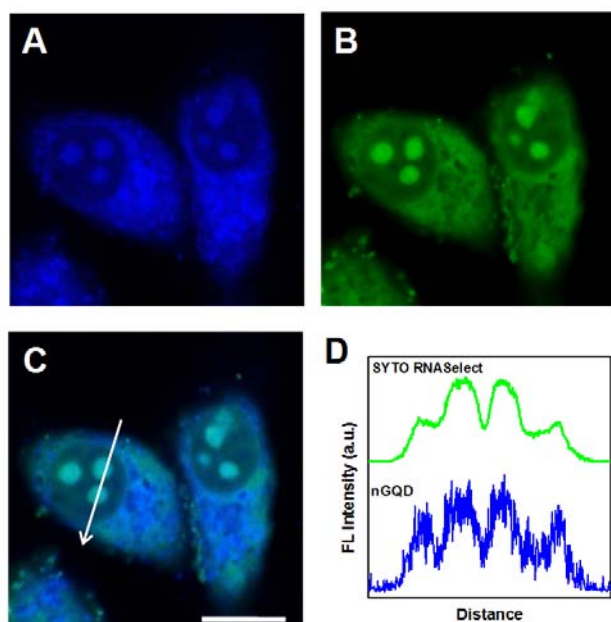


Fig. 4 Colocalization of nGQD and SYTO RNA-Select dye. Live HepG2 cells loaded with nGQD (400 μ g/mL) and SYTO RNA-Select dye (500nM) were fixed with paraformaldehyde and scanned under confocal microscope. (A) Fluorescence image recorded in the nGQD channel (λ_{ex} = 405 nm and fluorescence signal collected between 425nm and 475nm); (B) Fluorescence image recorded in the SYTO RNA-Select dye channel (λ_{ex} = 488 nm and the fluorescence signal collected between 500nm and 530nm); (C) The merged image of both channels (scale bar is 20 μ m); (D) Fluorescence intensity profile along the line shown in (C).

regions or the enhanced luminescence of nGQDs in the nucleolus when evenly distributed throughout the whole cells. Control experiments showed that the luminescence of nGQDs in buffer solution did not give out obvious change upon addition of DNA or RNA (spectra not provided), indicating that high concentration of nGQDs in the nucleolus may be important for the specific stain.

In order to prove that the physiological situations of the cells were not interfered during the stain processes, MTT assay was carried out to evaluate the cytotoxicity of nGQD. HepG2 cells were incubated together with nGQD or cGQD at various concentrations and the cell viability was quantified after 24h. As shown in Fig. S5, although the metabolic activity of the cells was slightly restricted when incubated with nGQD, the cells kept ~80 % viability after the treatment with very concentrated nGQD (750 μ g/mL). Since much shorter treating time and lower concentration (5 h and 400 μ g/mL) were applied for the stain process, nGQD could be considered as a nucleoli stain at an acceptable level of biocompatibility, which was consistent with the low cytotoxicity of nitrogen doped GQDs proved in the recent work.^{33, 34}

It should be noticed that unlike the nucleolar-targeting quantum dots introduced by Shen et al,¹⁸ where a large DNA-binding ligand was employed, the only difference between nucleoli-rich distributed nGQD and cytoplasm-only distributed cGQD was their surface group, which was primary amine and carboxyl acid, respectively. The varied subcellular distribution could therefore be attributed to the electrostatic attraction of the positively charged nGQD and the negative charged

nucleolar regions. The electrostatic interaction induced accumulation was also observed when the positively charged chitosan nanoparticles were applied to stain the nucleoli.³⁵ On the other side, in a previous work Qian et al had covalently linked diamine with carboxyl acid groups on their GQD but the modified GQD only localized in the cytoplasm as most of the other GQDs.³² Considering the small size of the dominating channel of nuclear pore complexes (~5.2 nm in diameter),³⁶ it was the large size of the GQD used in Qian et al's work (~10 nm in diameter) that prevented the transportation of their GQD through the nuclear envelope and consequently retained them in the cytoplasm. Based on these results, it is reasonable to suggest that the positively charged surface and the ultra-small size are the key parameters connected with the nucleoli stain property of our nGQD. This finding is of great significance for the development of functional nanomaterials targeting subcellular organelles. At the same time, detailed investigation on the uptake mechanism of nGQD should be desirable for understanding the toxicity of nanomaterials at the cellular and animal level.

Conclusions

We have demonstrated that a simple diamine coupling reaction can modulate the subcellular localization of GQDs from cytoplasm only to a nucleoli-rich distribution. Benefiting from the positively charged surface and the ultra-small size (2.5nm in diameter), a novel fluorescent probe, nGQD, has been successfully developed to light up the nucleoli of living cells. Compared with small organic dyes, the planar sheet of graphene structure is well kept in nGQD, which bestows this novel fluorophore a great advantage to combine the specific nucleoli localization with drug delivery and photothermal therapy functions of GQD.^{29,30} Work is currently under way in this regard.

Acknowledgements

This study was supported by the National Natural Science Foundation of China (21103230, 21273287, 21573289), Natural Science Foundation of Shandong Province (ZR2014BM028), Key R&D Program of Shandong province (2015GSF118013) and Fundamental Research Funds for the Central Universities (27R1504061A).

Notes and references

- 1 J. Yu, D. Parker, R. Pal, R. A. Poole and M. J. Cann, *J. Am. Chem. Soc.*, 2006, **128**, 2294-2299.
- 2 M. Carmo-Fonseca, L. Mendes-Soares and I. Campos, *Nat. Cell Biol.*, 2000, **2**, E107-E112.
- 3 M. M. Yusupov, G. Zh. Yusupova, A. Baucom, K. Lieberman, T. N. Earnest, J. H. D. Cate and H. F. Noller, *Science*, 2001, **292**, 883-896.

- 4 M. O. J. Olson, M. Dunder and A. Szebeni, *Trends Cell Biol.*, 2000, **10**, 189-196.
- 5 P. R. Kelemen, R. J. Buschmann and P. Weisz-Carrington, *Cancer*, 1990, **65**, 1017-1020.
- 6 M. Derenzini, *Micron*, 2000, **31**, 117-120.
- 7 R. Zhang, Z. Ye, Y. Yin, G. Wang, D. Jin, J. Yuan and J. A. Piper, *Bioconjugate Chem.*, 2012, **23**, 725-733.
- 8 N. A. O'Connor, N. Stevens, D. Samaroo, M. R. Solomon, A. A. Marti, J. Dyer, H. Vishwasrao, D. L. Akins, E. R. Kandel and N. J. Turro, *Chem. Commun.*, 2009, 2640-2642.
- 9 C. A. Puckett and J. K. Barton, *J. Am. Chem. Soc.*, 2009, **131**, 8738-8739.
- 10 K. Y. Zhang, S. P.-Y. Li, N. Zhu, I. W.-S. Or, M. S.-H. Cheung, Y.-W. Lam and K. K.-W. Lo, *Inorg. Chem.*, 2010, **49**, 2530-2540.
- 11 E. J. New, A. Congreve and D. Parker, *Chem. Sci.*, 2010, **1**, 111-118.
- 12 B. Zhou, W. Liu, H. Zhang, J. Wu, S. Liu, H. Xu and P. Wang, *Biosens. Bioelectron.*, 2015, **68**, 189-196.
- 13 X. Liu, Y. Sun, Y. Zhang, F. Miao, G. Wang, H. Zhao, X. Yu, H. Liu and W. Y. Wong, *Org. Biomol. Chem.*, 2011, **9**, 3615-3618.
- 14 G. Song, F. Miao, Y. Sun, X. Yu, J. Z. Sun and W.-Y. Wong, *Sens. Actuators, B*, 2012, **173**, 329-337.
- 15 G. Song, Y. Sun, Y. Liu, X. Wang, M. Chen, F. Miao, W. Zhang, X. Yu and J. Jin, *Biomaterials*, 2014, **35**, 2103-2112.
- 16 Z. Li, S. Sun, Z. Yang, S. Zhang, H. Zhang, M. Hu, J. Cao, J. Wang, F. Liu, F. Song, J. Fan and X. Peng, *Biomaterials*, 2013, **34**, 6473-6481.
- 17 J. Wang, S. Sun, D. Mu, J. Wang, W. Sun, X. Xiong, B. Qiao and X. Peng, *Organometallics*, 2014, **33**, 2681-2684.
- 18 R. Shen, X. Shen, Z. Zhang, Y. Li, S. Liu and H. Liu, *J. Am. Chem. Soc.*, 2010, **132**, 8627-8634.
- 19 L. Li, G. Wu, G. Yang, J. Peng, J. Zhao and J. J. Zhu, *Nanoscale*, 2013, **5**, 4015-4039.
- 20 J. Shen, Y. Zhu, X. Yang and C. Li, *Chem. Commun.*, 2012, **48**, 3686-3699.
- 21 X. T. Zheng, A. Ananthanarayanan, K. Q. Luo and P. Chen, *Small*, 2015, **11**, 1620-1636.
- 22 J. Peng, W. Gao, B. K. Gupta, Z. Liu, R. Romero-Aburto, L. Ge, L. Song, L. B. Alemany, X. Zhan, G. Gao, S. A. Vithayathil, B. A. Kaiparettu, A. A. Marti, T. Hayashi, J. J. Zhu and P. M. Ajayan, *Nano Lett.*, 2012, **12**, 844-849.
- 23 D. Pan, L. Guo, J. Zhang, C. Xi, Q. Xue, H. Huang, J. Li, Z. Zhang, W. Yu, Z. Chen, Z. Li and M. Wu, *J. Mater. Chem.*, 2012, **22**, 3314-3318.
- 24 X. Wu, F. Tian, W. Wang, J. Chen, M. Wu and J. X. Zhao, *J. Mater. Chem. C*, 2013, **1**, 4676-4684.
- 25 V. Kumar, V. Singh, S. Umrao, V. Parashar, S. Abraham, A. K. Singh, G. Nath, P. S. Saxena and A. Srivastava, *RSC Advances*, 2014, **4**, 21101-21107.
- 26 Y. Dong, C. Chen, X. Zheng, L. Gao, Z. Cui, H. Yang, C. Guo, Y. Chi and C. M. Li, *J. Mater. Chem.*, 2012, **22**, 8764-8766.
- 27 W. Shang, X. Zhang, M. Zhang, Z. Fan, Y. Sun, M. Han and L. Fan, *Nanoscale*, 2014, **6**, 5799-5806.
- 28 S. Zhu, J. Zhang, C. Qiao, S. Tang, Y. Li, W. Yuan, B. Li, L. Tian, F. Liu, R. Hu, H. Gao, H. Wei, H. Zhang, H. Sun and B. Yang, *Chem. Commun.*, 2011, **47**, 6858-6860.
- 29 X. Wang, X. Sun, H. He, H. Yang, J. Lao, Y. Song, Y. Xia, H. Xu, X. Zhang and F. Huang, *J. Mater. Chem. B*, 2015, **3**, 3583-3590.
- 30 X. Wang, X. Sun, J. Lao, H. He, T. Cheng, M. Wang, S. Wang and F. Huang, *Colloids and surfaces. B, Biointerfaces*, 2014, **122**, 638-644.
- 31 S. Zhu, J. Zhang, S. Tang, C. Qiao, L. Wang, H. Wang, X. Liu, B. Li, Y. Li, W. Yu, X. Wang, H. Sun and B. Yang, *Adv. Funct. Mater.*, 2012, **22**, 4732-4740.
- 32 Z. Qian, J. Ma, X. Shan, L. Shao, J. Zhou, J. Chen and H. Feng, *RSC Advances*, 2013, **3**, 14571-14579.
- 33 Q. Liu, B. Guo, Z. Rao, B. Zhang and J. R. Gong, *Nano Lett.*, 2013, **13**, 2436-2441.
- 34 Y. Zhao, Q. Liu, S. Shakoor, J. R. Gong and D. Wang, *Toxicology Research*, 2015, **4**, 270-280.
- 35 K. Wang, X. Yuan, Z. Guo, J. Xu and Y. Chen, *Carbohydr. Polym.*, 2014, **102**, 699-707.
- 36 D. Mohr, S. Frey, T. Fischer, T. Güttler and D. Görlich, *The EMBO Journal*, 2009, **28**, 2541-2553.

Table of Contents

A novel graphene quantum dot capable of lighting up the nucleoli of living cells has been developed.

